

Published in final edited form as:

Nat Cell Biol. 2008 June ; 10(6): 688–697. doi:10.1038/ncb1731.

STIM1 signaling controls store operated calcium entry required for development and contractile function in skeletal muscle

Jonathan Stiber^{1,*}, April Hawkins^{1,*}, Zhu-Shan Zhang^{1,*}, Sunny Wang¹, Jarrett Burch¹, Victoria Graham¹, Cary C. Ward¹, Malini Seth¹, Elizabeth Finch¹, Nadia Malouf², R. Sanders Williams¹, Jerry P. Eu¹, and Paul Rosenberg^{1,#}

¹ Department of Medicine, Duke University School of Medicine, Durham, NC

² Department of Pathology, University of North Carolina, Chapel Hill, NC

Abstract

It is now well established that stromal interaction molecule 1 (STIM1) is the calcium sensor of endoplasmic reticulum (ER) stores required to activate store-operated calcium entry (SOC) channels at the surface of non-excitable cells. Yet little is known about STIM1 in excitable cells such as striated muscle where the complement of calcium regulatory molecules is rather disparate from that of non-excitable cells. Here, we show that STIM1 is expressed in both myotubes and adult skeletal muscle. Myotubes lacking functional STIM1 fail to exhibit SOC and fatigue rapidly. Moreover, mice lacking functional STIM1 die perinatally from a skeletal myopathy. In addition, STIM1 haploinsufficiency confers a contractile defect only under conditions where rapid refilling of stores would be needed. These findings provide novel insight to the role of STIM1 in skeletal muscle and suggest that STIM1 has a universal role as an ER/SR calcium sensor in both excitable and non-excitable cells.

Store-operated calcium entry (SOC) is a well established mechanism to refill internal calcium stores in many types of cells. Refilling of internal calcium stores depends on an endoplasmic reticulum (ER) calcium sensor that was recently identified as Stromal Interaction Molecule 1 (STIM1)^{1,2}. STIM1 is a single-pass transmembrane phosphoprotein located in the membrane of the ER, where it interacts with SOC channels in the plasma membrane³. Following the release of stored calcium, STIM1 molecules sense internal store depletion and aggregate at sites within the ER (called punctae) in close proximity (10–15 nm) to SOC channels located in the plasma membrane^{4–6}. STIM1 punctae thus serve as critical links between internal calcium stores and SOC channels on the plasma membrane⁷. STIM1-dependent SOC is important for many cell processes, including calcium-dependent gene expression.

STIM1 influences the activity of several different types of calcium channels including store-operated (Orai1 and TRPC1/4 channels) and receptor-operated channels (TRPC3/6 and ARC channels)⁸. Orai1 has been shown to be required for store-operated calcium entry by genome-wide screens, and STIM1 is needed to activate Orai channels^{9,10}. Recent work has also identified several TRP channels and ARC channels as STIM1-regulated channels that are activated following agonist stimulation in non-excitable cells^{11,12}. Orai (CRACM) family members (Orai1–3) form highly selective calcium channels with the characteristics of I_{crac} when co-expressed with STIM1. In contrast, Orai channels co-expressed with STIM2 display both store-operated and store-independent gating¹³. Orai1 may also exist in a complex with transient receptor potential channels (TRPC1) where, together, STIM1, Orai1 and TRPC1 form

#For correspondence: Paul Rosenberg, 4321 Medical Park Drive, Suite 200, Durham, NC 27704, 919-479-2315, 919-477-0650, E-mail: rosen029@mc.duke.edu.

*Denotes equal contribution

store-operated channels as has been described in epithelial cells of salivary glands¹⁴. STIM1 has also been shown to influence TRPC1 channel gating through a direct interaction that requires the C-terminal ERM or lysine rich region^{12, 15}. Finally, STIM1 can also influence other TRPC channels through an indirect mechanism that requires TRPC1, as silencing STIM1 reduced TRPC3 currents¹². Thus, it seems clear that STIM1 is required as part of a more general mechanism to activate plasma membrane calcium entry channels of several types.

While substantial evidence supports the critical role of STIM1 signaling in regulating SOC in non-excitabile cells, far less is known about SOC in excitable cells such as striated muscle, where huge fluctuations in cellular calcium are required for muscle contraction¹⁶. Muscle contraction requires excitation-contraction (EC) coupling, a process whereby changes in the membrane potential evoke release of the SR calcium stores by the ryanodine receptor (RYR1). Refilling of internal stores for EC coupling was previously thought to occur exclusively through the resequestration of calcium by the highly efficient calcium pumps (SERCA) located in the SR membrane¹⁷. However, SOC was recently shown to exist in myofibers where it can be activated rapidly in response to store-depletion¹⁸.

It is thought that the fundamental role for SOC in muscle is to refill internal calcium stores to ready the myofiber for subsequent muscle contraction¹⁹. Defects in muscle SOC are believed to lead to muscle fatigue and exercise intolerance²⁰. However, we recently proposed that SOC is also necessary to maintain NFAT transactivation during both muscle development and the remodeling response to exercise^{19, 21}. In this context, we hypothesize that NFAT transactivation through sustained SOC confers a form of memory of recent neurostimulation to the trained muscle. The identification of STIM1 as the sensor of calcium store depletion allowed for the generation of a genetic model to test our hypothesis that SOC provides a pool of calcium required not only for skeletal muscle contraction, but also for muscle development and remodeling.

RESULTS

We pursued studies of STIM1 to assess a previously unrecognized role for this protein in skeletal muscle, where SOC is necessary for NFAT translocation and NFAT signaling is known to play an important role in myogenesis and in the adaptation to exercise (*see* Supplemental information Fig. s1a)^{19, 22, 23}. We first analyzed the spatial and temporal expression pattern for STIM1 during myogenesis. We found that STIM1 is expressed at low levels in myoblasts, but that its expression is increased following differentiation into multinucleated myotubes (Fig. 1A). Interestingly, STIM1 redistributes from a peri-nuclear localization in myoblasts to the cell periphery of differentiated myotubes (Fig. 1B–C). This localization of STIM1 near the plasma membrane appears to occur under basal conditions even when stores are fully loaded with calcium, unlike the redistribution of STIM1 to the cell periphery following store depletion in non-excitabile cells^{4, 24}. The STIM1 redistribution appears to be a unique feature of myotubes and may reflect the spontaneous calcium release required for myogenesis. Consistent with the increase in STIM1 expression and its peripheral location in myotubes, the rate of Ba²⁺ entry (a surrogate for Ca²⁺ entry) in myotubes was 4–5 times faster (2.72×10^{-3} arbitrary units/second), than in myoblasts (5.57×10^{-4} arbitrary units/second) ($p < 0.001$) (Fig. 1D and E). In addition, myotubes overexpressing a wildtype (WT) or a constitutively active form of STIM1¹ displayed an increase (2.5 and 4.5 fold respectively) in basal NFAT transactivation when compared to myotubes expressing endogenous STIM1 or compared to myotubes in which STIM1 expression was silenced using an shRNA plasmid directed against mouse STIM1 (*see* Supplemental Information Fig. s1B–D). These data suggest that differentiation signals upregulate STIM1 in skeletal myotubes which is correlated with greater SOC. Moreover, myotubes overexpressing WT STIM1 or a constitutively active form of STIM1 (D76A) show enhanced NFAT-dependent transcriptional regulation during myogenesis (Fig. s1B).

Calcineurin/NFAT signaling controls morphogenetic events of muscle formation, which occur around embryonic day 15.5 (E15.5)^{25–27}. STIM1 mRNA expression increases in the embryo starting at E7.5 through E15.5: concomitant with this period are morphogenetic events that are controlled by NFAT transactivation (see Supplemental Information Fig. s2A). A STIM1 specific probe detected STIM1 mRNA by *in situ* hybridization in the embryonic limbs and brain at E16.5 (see Supplemental Information Fig. s2 B–D), whereas the sense probe failed to detect any signal (see Supplemental Information Fig. s2 C–E). Thus, results of these *in vitro* and *in vivo* studies indicate STIM1 may have relevant role in muscle differentiation.

We next established a loss of function model for STIM1 using a gene-trap approach that results in expression of a STIM1-LacZ fusion protein under the control of the endogenous STIM1 promoter (ES cell line RRS558) (Fig. 2A–C). The STIM1-LacZ fusion protein leaves the N-terminal SAM and EF hand domains of the native STIM1 protein intact, but disrupts the ERM coiled-coiled domains that are required for SOC activation^{15, 28}. The localization of the STIM1-LacZ fusion protein in STIM1^{+gt} heterozygous mice can thus be used to determine which cells express the endogenous STIM1 protein. We detected the STIM1-LacZ fusion protein in all muscle groups that were harvested from STIM1^{+gt} heterozygous mice, and also in the Purkinje neurons of the cerebellum and in a selected subset of cells of the spleen and thymus (see Supplemental Information Fig. s3A–E). Intercrossing STIM1^{+gt} heterozygotes revealed neonatal lethality affecting most STIM1^{gt/gt} animals before weaning (Table 1). Surviving STIM1^{gt/gt} mice exhibited a significant reduction in body weight, hypotonia of the lower limbs on hindlimb suspension, and generalized fatigue (Fig 2D). Embryos harvested between E11.5 and E16.5 revealed normal Mendelian ratios for STIM1^{gt/gt} mice (25%), but only ten percent of neonates examined between P0 to P7 were STIM1^{gt/gt}, indicating late fetal or neonatal demise.

Primary myotubes were isolated from STIM1^{+/+}, STIM1^{+gt} and STIM1^{gt/gt} mice to determine whether deleting the C-terminus of STIM1 affected SOC. SOC, as assessed using the rate of Ba⁺² entry, was significantly reduced in Fura-2 loaded myotubes from STIM1^{gt/gt} and STIM1^{+gt} mice (1.62×10^{-4} and 2.92×10^{-3} arbitrary units/sec respectively) compared to STIM1^{+/+} myotubes (7.0×10^{-3} arbitrary units/sec) (Fig 2E–F). These studies demonstrate that the mutation in the STIM1 gene results in a loss of function model.

We analyzed the properties of SOC currents (I_{soc}) in primary myotubes isolated from STIM1^{+/+}, STIM1^{+gt} and STIM1^{gt/gt} mice using whole-cell patch-clamp recording. For these studies, we used recording solutions and protocols that are standard for recording I_{soc} in other cells^{29, 30} and SOC was activated by depleting calcium stores with the SERCA antagonist thapsigargin (2μM) (Fig. 3A). SOC currents were analyzed from 33 STIM1^{+/+} myotubes that exhibited a voltage-gated Na⁺ current. SOC currents recorded from these myotubes displayed current-voltage relationships with two distinct patterns: an inwardly rectifying current (19/33 cells) and a linear current (14/33 cells) (Fig. 3A–C, and Fig. s4A–C, respectively). The inwardly rectifying current displayed a current density at –80mV of –5.05 pA/pF for STIM1^{+/+} and –1.98 pA/pF for STIM1^{+gt} myotubes. In contrast, store depletion with thapsigargin (2μM) evoked little change in the current density in STIM1^{gt/gt} myotubes. The inwardly rectifying currents recorded from STIM1^{+/+} and STIM1^{+gt} myotubes resembled SOC currents recorded in other systems³¹ and were therefore studied in greater detail. The myotube SOC current was as permeable to barium (98%) or cesium (90%) as to calcium (Fig 3D and E), which is consistent with the ion selectivity profile of SOC channels³². Moreover, switching the external solution from 2 mM calcium to a divalent-free solution resulted in a large increase in the current amplitude (278% control) (Fig 3D–E), indicating an increase in the permeability of monovalent cations in the absence of Ca⁺², which is another hallmark of SOC currents. Finally, myotube SOC currents were inhibited by the trivalent cation Gd⁺³ (10 μM) (Fig. 3D–E) and the compound SKF96566 (10 μM) (not shown). These findings suggest that the SOC currents

recorded from $STIM1^{+/+}$ myotubes resemble calcium release activated calcium (CRAC) currents recorded from many non-excitable cells^{33, 34}. The linear currents that were recorded from a subset of myotubes suggest that, in addition to (classic) CRAC-like SOC currents, other plasma membrane currents may also be activated following store depletion in skeletal myotubes. Although the nature of these currents is currently unknown, future studies to further characterize the currents activated by store depletion in skeletal myotubes will more fully define the mechanism(s) underlying SOC in these excitable cells. It is possible, for example, that the observation of a linear current in some myotubes and an inwardly rectifying current in other myotubes may reflect differences in the complement of channels that are activated by store depletion in these two populations of myotubes and may also reflect differences in SOC currents between excitable cells and non-excitable cells.

We next examined the localization of STIM1 in skeletal muscle from the hindlimbs of adult mice. Immunostaining for STIM1 using two independent antibodies displayed a striated pattern that partially co-localized with the RYR channels that are known to be present at the terminal cisternae (Fig. 4A–C). These studies suggested that STIM1 may localize to the skeletal myofiber SR. We next examined STIM1 expression in subcellular fractions of rabbit skeletal muscle. Isolated microsomal fractions were obtained using sucrose gradients and revealed STIM1 expression in fractions corresponding to the t-tubule, longitudinal SR, and the terminal cisternae (Fig. 4F). We also examined the expression of the STIM1-LacZ fusion protein by electron microscopy (Fig. 4D–E). Aggregates of the reaction products of beta-galactosidase were detected in the longitudinal SR as well as the junction of the t-tubule and terminal cisternae. The STIM1-LacZ aggregates were detected in the majority of, but not all, foot processes, which is mostly likely because we examined only $STIM1^{+/gt}$ muscles. These results provide insight into the structure of SOC complex in muscle and may explain differences in SOC kinetics that we and others have observed in myofibers compared to non-excitable cells³⁵.

We next carried out a series of studies to investigate how the loss of STIM1 affects skeletal muscle structure and function. Histological sections of muscles from $STIM1^{gt/gt}$ mice revealed increased central nucleation (*see* Supplemental Information Fig. s5A–C), a hallmark of a congenital myopathy. In addition, dystrophin staining of muscles from $STIM1^{gt/gt}$ mice revealed markedly reduced muscle cross sectional area compared to $STIM1^{+/+}$ mice (Fig 5A–B). Ultrastructural analysis of *tibialis anterior* (TA) muscle of $STIM1^{gt/gt}$ mice using transmission electron microscopy revealed markedly swollen mitochondria in the subsarcolemmal and intramyofibrillary space compared to control $STIM1^{+/+}$ littermates (Fig. 5C–D, $STIM1^{gt/gt}$, and Fig. 5E, $STIM1^{+/+}$). These ultrastructural abnormalities in muscles of $STIM1^{gt/gt}$ mice were also associated with altered expression of muscle specific proteins of the SR and sarcomere (Fig. 6A). There was a marked decrease in the expression of SERCA1 and myosin heavy chain in hindlimb muscles from $STIM1^{gt/gt}$ neonatal mice, supporting the histological evidence of muscle damage.

Based on these indications of muscle pathology, we hypothesized that the perinatal lethality in $STIM1^{gt/gt}$ is due to a congenital myopathy. To test our hypothesis, we assessed the physical and functional characteristics of skeletal muscle from $STIM1^{+/gt}$ mice as well. Although sarcomeric architecture was basically preserved, foot processes appeared intact, and the weights, lengths and single twitch contractions of isolated extensor digitorum longus (EDL) muscles evoked with stimulation at 60 and 80 mV were not different between eight-week old $STIM1^{+/gt}$ and $STIM1^{+/+}$ mice (not shown), force frequency measurements of isolated EDL muscles³⁶ from $STIM1^{+/+}$ and $STIM1^{+/gt}$ mice revealed an inability of $STIM1^{+/gt}$ muscles to generate the same level of tetanic forces as $STIM1^{+/+}$ mice (Fig. 6D–E). Moreover, EDL muscles isolated from $STIM1^{+/gt}$ mice displayed a marked reduction in the time to fatigue as compared to those taken from $STIM1^{+/+}$ mice (24 ± 4.7 sec vs. 35.6 ± 0.5 sec, $p < 0.002$) (Fig

6F). Taken together, these results suggest that muscles from $STIM1^{+/gt}$ mice display severe defects in force generation and fatigue resistance and support the notion that neonatal $STIM1$ mutant mice manifest significant muscle weakness.

Refilling of internal calcium stores following membrane depolarization has long been recognized to occur through the rapid action of the calcium pump (SERCA) located in the longitudinal SR³⁷. However recent evidence that store-operated calcium influx is required to refill internal stores has implicated SOC in the regenerative calcium oscillations observed in muscle and suggests that SOC is required to prevent muscle fatigue²⁰. Calcium oscillations in myotubes depend in part on calcium entry and may play a role in regulating gene expression during muscle differentiation^{21, 38, 39}. We therefore examined KCl-evoked calcium transients from $STIM1^{+/+}$, $STIM1^{gt/+}$ and $STIM1^{gt/gt}$ myotubes. While a single KCl-evoked calcium transient was not significantly different between $STIM1^{+/+}$, $STIM1^{gt/+}$ and $STIM1^{gt/gt}$ myotubes, indicating comparable levels of internal calcium stores, a train of KCl pulses resulted in a rapid decrement in the amplitude of subsequent calcium transients in $STIM1^{+/gt}$ and $STIM1^{gt/gt}$ myotubes. Control $STIM1^{+/+}$ myotubes responded to subsequent KCl-pulses with a minor decrement in calcium transient amplitude (Fig. 7A–D). At the end of each KCl stimulation protocol, we measured the SR calcium store content by depleting stores with thapsigargin (2 μ M) and caffeine (10 mM) and found that $STIM1^{+/gt}$ and $STIM1^{gt/gt}$ myotubes showed significant defects in refilling of internal stores compared to $STIM1^{+/+}$ myotubes (Fig. 7E). These results indicate that SOC is needed to refill internal calcium stores in a muscle that is subjected to repeated stimulation, in order to prepare for the next depolarization.

DISCUSSION

In this study, we provide evidence that mice carrying mutant $STIM1$ have defects in muscle differentiation and in muscle contractile activity. We find that neonatal mice lacking functional $STIM1$ -dependent SOC die from a perinatal myopathy and that haploinsufficiency of $STIM1$ in adult mice confers increased susceptibility to fatigue. These findings support a model where $STIM1$ is required to activate SOC and refill internal stores in myotubes in response to signals associated with muscle differentiation and in myofibers subjected to increased motor nerve activity. Although the precise signals are not known at this point, it is likely that $STIM1$ -mediated SOC is important for both short term calcium responses, i.e. muscle contraction, and long term responses such as a remodeling through calcium dependent gene expression.

In this work, we provide evidence that $STIM1$ is critical for myotube development and that the loss of $STIM1$ results in defective SOC, which underlies defective muscle differentiation both *in vitro* and *in vivo*. $STIM1$ expression increased during myotube differentiation and correlated with increased SOC activity in myotubes compared to myoblasts. $STIM1$ -dependent SOC plays an important role in NFAT dependent gene expression as was evident from $STIM1$ gain and loss of function studies in C_2C_{12} cells. It is also likely that $STIM1$ -dependent store refilling is important to maintain calcium oscillations that are needed for muscle differentiation⁴⁰. For example, $STIM1^{gt/gt}$ myotubes fail to exhibit SOC in response to thapsigargin induced SR store depletion or in response to repeated KCl-pulses. Moreover, $STIM1^{+/+}$ myotubes exposed to a series of depolarizing signals maintain full calcium stores, while $STIM1^{gt/gt}$ myotubes fail to refill their stores. These results suggest that $STIM1$ is important for store refilling following calcium release from RYR1-containing calcium stores by membrane depolarization, which is important for muscle differentiation⁴¹.

In mature muscle, we found that $STIM1$ haploinsufficiency confers a contractile defect only under conditions of increased contractile demand, where calcium store depletion is most likely to occur. Under these conditions of increased muscle usage, $STIM1$ haploinsufficiency likely

results in ineffective sensing of store depletion that occurs with high frequency stimulation, thus resulting in a defect in force generation and early fatigue. In the present study we were unable to distinguish whether the increased fatigue results from defective refilling of RYR1-containing calcium stores or a developmental defect. We did find, however, that muscles from $STIM1^{gt/gt}$ mice expressed reduced levels of SERCA1 and myosin heavy chain. Reduced expression of either of these proteins might result in reduced muscle performance. Taken together, these studies of $STIM1$ mutant mice indicate that SOC is an important calcium signaling pathway in muscle operating to refill calcium stores needed for muscle contraction.

We found that $STIM1$ is localized to the muscle SR where calcium is released by RYR1 and refilled by SERCA1. In fact, $STIM1$ localizes to both the foot process and longitudinal SR. It is possible, therefore, that SOC is important in muscle to augment EC coupling, through a mechanism in which $STIM1$ senses the depletion of RYR stores with augmented contractile activity, activates SOC channels in the t-tubule membrane, and thus increases calcium store refilling. In this way, $STIM1$ may function as a sensor of contractile stress. In this model, muscles under ambient conditions would cycle calcium through the RYR calcium stores in rapid fashion; however muscles under conditions of increased motor nerve activity would activate $STIM1$ -dependent SOC to rapidly refill internal stores. SOC would provide a sustained increase in subsarcolemmal calcium that would set in motion a series of remodeling events aimed at optimizing muscle performance. This muscle remodeling might include the upregulation of TRPC3 channel expression that serves to augment SOC with subsequent bouts of exercise¹⁹. Interestingly, recent reports suggest that $STIM1$ can interact with TRPC1 and indirectly with TRPC3 channels to mediate SOC in diverse cell types^{12, 15, 42, 43}. The findings presented here provide the first genetic evidence for essential physiological functions of SOC in skeletal muscle and validate a conceptual model whereby SOC confers cellular memory of recent motor nerve activity. In this way, $STIM1$ -dependent SOC in muscle provides a mechanism to sustain increases in $[Ca^{+2}]_c$ in order to preserve contractile function during repeated contractions and to activate calcium-dependent signaling events that underlie remodeling responses associated with neurostimulation.

SOC has been recognized as mechanism of calcium overload in skeletal myopathies such as muscle dystrophy^{44–46}. Yet the only physiological functions known to date for $STIM1$ and $Orai1$ have been revealed by mutations in human $Orai1$ gene, where a defect in SOC leads to severe combined immunodeficiency, and in *C. elegans* mutants, where mutations in $STIM1$ and $Orai$ homologues lead to abnormal gut function and infertility^{47, 48}. However, one patient with a mutation in $Orai1$ also manifests a skeletal myopathy that may involve impaired calcineurin/NFAT signaling (3). Moreover, $Orai1$ reporter mice indicate the robust expression of $Orai1$ in mature skeletal muscle⁴⁹. Here we provide direct evidence that loss of $STIM1$ in mice produces a skeletal myopathy. Taken together, these studies indicate that $STIM1$ participates in a conserved calcium signaling network that is active in diverse cell types which utilize calcineurin signaling to respond to changing environmental stimuli.

METHODS

Cell culture

C_2C_{12} cells were propagated in Dulbecco's Modified Eagle Medium (DMEM)-low glucose media supplemented with 10% fetal bovine serum (FBS) and 100U/mL penicillin-streptomycin. C_2C_{12} differentiation from myoblasts to myotubes took place over 5 days while incubated in differentiating media (DM) containing DMEM-high glucose media with 2% horse serum, 10 μ g/mL transferrin, 10 μ g/mL insulin, 50mM HEPES buffer pH 7.4, 100 U/mL penicillin-streptomycin. Experiments involving C_2C_{12} cells were performed after 5 days in DM except when otherwise noted. Primary myoblasts were isolated from $STIM1^{gt/gt}$, $STIM1^{+/gt}$, and $STIM1^{+/+}$ neonates by collagenase digestion using a previously described

protocol and subsequently allowed to differentiate into myotubes as described above for C₂C₁₂ cells⁵⁰.

[Ca²⁺]_i imaging

C₂C₁₂ cells were plated on 0.1% gelatin-coated glass coverslips at least 12 hours prior to imaging. Imaging of myotubes was performed after switching over to differentiating media for 5 days. Ca²⁺ imaging was performed with a 40 X objective on an automated fluorescence microscope with a Photometrics CoolSnap camera. C₂C₁₂ cells were loaded with 10 μM Fura-2-acetoxymethyl ester in extracellular buffer (140 mM NaCl, 2.8 mM KCl, 2 mM CaCl₂, 2 mM MgCl₂, 10 mM glucose, and 10 mM HEPES) for 30 minutes at room temperature while shielded from light. Fura-2 fluorescence was measured by illuminating the cells with an alternating 340/380 nm light every 1–2 seconds and fluorescent images were captured at 510 nm. Changes in intracellular Ca²⁺ concentration were derived from changes in the ratio of fluorescent intensity at 340 and 380 nm. For Ca²⁺ add-back experiments, C₂C₁₂ cells were bathed in Ca²⁺-free media (140 mM NaCl, 2.8 mM KCl, 4 mM MgCl₂, 10 mM glucose, 10 mM HEPES, and 10 mM EGTA), and then treated with 2 μM of thapsigargin and 10 μM of verapamil, followed by 2 mM barium after Ca²⁺ store depletion.

Immunohistochemistry

C₂C₁₂ cells were fixed as myoblasts or myotubes with ice-cold methanol at –20 °C for 10 minutes. Immunostaining with anti-STIM1 antibody (BD Biosciences) was performed at a dilution of 1:100. Images were obtained with a 40x objective on Zeiss-LSM 510 META fluorescence microscope and analyzed with MetaMorph software (Universal Imaging). For immunofluorescence studies of muscle tissues, muscles were frozen in OCT and then cryosectioned. Images were obtained using a 40X objective on a Zeiss LSM 510 inverted confocal microscope. Rabbit anti-RYR1 antibody was obtained from Dr. Gerhard Meissner (UNC Chapel Hill).

Whole-cell Patch-Clamp Recordings

Patch clamp experiments were performed to record currents in the whole cell mode with pipettes filled with solutions containing 137 mM cesium aspartate, 2 mM CsCl, 8 mM MgSO₄, 15 mM HEPES, 12 mM BAPTA, pH 7.2 (with CsOH), 310 mOsm (with d-Mannitol). The external solution consisted of 150 mM NaCl, 2 mM CaCl₂, 1 mM MgCl₂, 10 mM HEPES, 10 mM glucose, 20 mM sucrose, pH 7.4 (with NaOH), 320 mOsm (with d-mannitol); in NMDG solution, Na⁺ was replaced with equivalent concentration of NMDG; in Ba²⁺ solution, Ca²⁺ replaced by Ba²⁺; in divalent -free (DVF) solution, Ca²⁺ and Mg²⁺ were omitted and 10mM EDTA was added. To block the L-type Ca²⁺ channel, verapamil (10μM) was added in external solutions; K⁺ channel blocked by Cs⁺ in the internal solution; and the voltage-dependent Na⁺ channel was inactivated by the stimulation protocol. The osmolarity of each solution was verified with a freezing-point osmometer (Advanced Instruments). Voltage across the cell attached membrane patch was controlled and currents recorded using an Axonpatch-200A amplifier with Digidata 1200 interface and analyzed with pCLAMP software. Currents were induced by 200 ms voltage ramp protocols every 2 seconds (1 mV/ms, from 100mV to –100mV), at a holding potential 0mV. Experiments were performed at room temperature with a sample rate of 4 kHz (filter 2 kHz). For analysis of I_{soc}, the first ramps before activation of SOC currents (usually 1–3) were pooled and used for leak-subtraction of all subsequent current recordings.

Antibodies and western blotting

Cell extracts were prepared by washing the cells with PBS and then extracting proteins with lysis buffer: PBS, 5mM EDTA, 5mM EGTA, 1mM sodium vanadate, 10mM sodium

pyrophosphate, 50mM sodium fluoride, and 1% Triton X-100. Proteins were resolved on SDS-polyacrylamide gels and electroblotted onto nitrocellulose membranes (Amersham Biosciences, Hybond-C Extra). After transfer, nitrocellulose membranes were blocked for 1 hour at room temperature in 5% milk with Tris-buffered saline/Tween 20 (TBST): 10mM Tris HCl, pH 8.0, 150mM NaCl, 0.1% Tween 20. Next, the membranes were incubated overnight at 4°C with anti-STIM1 primary antibody (BD Biosciences) diluted 1:250 with 1% milk in TBST. After washing with TBST, membranes were incubated at room temperature for 1 hour with secondary antibody. Peroxidase activity was visualized with enhanced chemiluminescence (Amersham Biosciences, ECL Advance™ Western Blotting Detection Kit). SERCA1 and MyoD antibodies were obtained from Affinity Bioreagents. Unless otherwise stated, equal loading was confirmed by immunoblotting with alpha-tubulin Ab (Santa Cruz).

STIM1 Gene Silencing

DNA templates for the synthesis of silencing RNA were cloned into an expression plasmid for subsequent transfection. The selection of the coding sequence for targeting STIM1 mRNA was done by using the siRNA Target Finder and Design Tool from Ambion. The potential target sequence was subjected to a BLAST search against mouse EST libraries to ensure specificity of the target. The oligonucleotide sequences were: *si-4* construct, sense, 5' GACCTCAATTACCATGACC 3', antisense, 3' CTGGAGTTAATGGTACTGG 5'; *si-6* construct, sense, 5' CCGTTACTCTAAGGAGCAC 3', antisense 3' GGCAATGAGATTCCTCGTG 5'. C₂C₁₂ myocytes were transfected using Fugene reagent (Roche).

STIM1-targeted mice

The ES cell line RRS558 from BayGenomics was generated by using a gene trap protocol with pGT0Lxf vector containing the engrailed 2 gene and β-galactosidase/neomycin-resistance fusion protein. A comparison between the BayGenomics database and the NCBI UniGene database suggested that the insertion site for this gene-trap construct is in exon 8 of STIM1, which corresponds to a fusion protein consisting of the extracellular and transmembrane domain of STIM1 with a β-galactosidase protein on the N terminus. A PCR based strategy was used to map the exact location that the gene-trap construct inserted into the STIM1 gene. Genotyping of littermates using tail digest genomic DNA first involved amplifying the LacZ gene to identify the mice with a targeted allele and then a second round of PCR using primers specific to the insertion site of the gene-trap construct was performed to identify homozygous mice.

β-galactosidase staining

All mouse tissues were dissected with cold PBS and immediately fixed with 4% PFA at 4°C for 1 hour. After rinsing the tissues with rinsing solution (5 mM EGTA, 0.01% deoxycholate, 0.02% NP40, 2 mM MgCl₂) 3 × 15 minutes at room temperature, the tissues were incubated in the dark with staining solution (5 mM K₃Fe(CN)₆, 5 mM K₄Fe(CN)₆, 5 mM EGTA, 0.01% deoxycholate, 0.02% NP40, 2 mM MgCl₂, 1 mg/mL X-gal solution) at 37°C until desired intensity was reached. The specimens were then washed with PBST, post-fixed with 4% PFA overnight, and then stored in 70% EtOH. Paraffin sectioning of the stained organs was performed by standard methods and subsequently stained with H&E. For electron microscopy of STIM1^{gt/+} muscle, samples were post-fixed in 2% PFA and 2% glutaraldehyde in 0.1 M cacodylate buffer pH7.4 for 12 hours. Sections were fixed in 1% OSO₄ and embedded in an epoxy resin mixture. Ultrathin sections were studied with an EM 410 electron microscope (Phillips). For control experiments STIM1^{+/+} samples were processed as above.

Skeletal Muscle Contractility and Fatigability

STIM1^{+/-gt} and STIM1^{+/-+} control mice were anesthetized and intact EDL muscles were removed and placed in Krebs buffer (pH 7.4). The intact whole muscles were placed in a 30 ml chamber between platinum stimulating electrodes and bathed in Krebs buffer continuously aerated with 95% O₂. The force transducer measurements were recorded and analyzed on computer using Polyview software (Grass, West Warwick, RI). Muscles were subjected to multiple frequencies of stimulation of 200 msec duration to produce the force-frequency relationship. Muscles were fatigued by stimulation at the frequency which produces maximum tetanic force, as well as submaximal frequencies, at 1 second intervals for 5 minutes while recording the changes in force production over time. All animal studies were performed under an approved IACUC protocol.

Supplementary Material

Refer to Web version on PubMed Central for supplementary material.

Acknowledgments

Special thanks to Dr. Mary Hutson for her guidance on whole mount *in situ* hybridization and imaging techniques and to Dr. Margaret Kirby's lab for providing imaging equipment. We would thank Drs. Gerhard Meissner and Qui-An Sun for their help with microscopical preparations. This research was done at the Sarah W. Stedman Nutrition and Metabolism Center at Duke University and supported by the following grants: a HHMI Physician-Scientist Early Career Award and NIH award (K08-HL077520) (JAS), NIH award (K08-HL-071841-04) (PBR), Mandel Foundation award (PBR), MDA research award (PBR), and a HHMI Training Fellowship for Medical Students (SW).

References

- Liou J, et al. STIM is a Ca²⁺ sensor essential for Ca²⁺-store-depletion-triggered Ca²⁺ influx. *Curr Biol* 2005;15:1235–1241. [PubMed: 16005298]
- Roos J, et al. STIM1, an essential and conserved component of store-operated Ca²⁺ channel function. *The Journal of cell biology* 2005;169:435–445. [PubMed: 15866891]
- Zhang SL, et al. STIM1 is a Ca²⁺ sensor that activates CRAC channels and migrates from the Ca²⁺ store to the plasma membrane. *Nature* 2005;437:902–905. [PubMed: 16208375]
- Luik RM, Wu MM, Buchanan J, Lewis RS. The elementary unit of store-operated Ca²⁺ entry: local activation of CRAC channels by STIM1 at ER-plasma membrane junctions. *The Journal of cell biology* 2006;174:815–825. [PubMed: 16966423]
- Wu MM, Buchanan J, Luik RM, Lewis RS. Ca²⁺ store depletion causes STIM1 to accumulate in ER regions closely associated with the plasma membrane. *The Journal of cell biology* 2006;174:803–813. [PubMed: 16966422]
- Liou J, Fivaz M, Inoue T, Meyer T. Live-cell imaging reveals sequential oligomerization and local plasma membrane targeting of stromal interaction molecule 1 after Ca²⁺ store depletion. *Proceedings of the National Academy of Sciences of the United States of America* 2007;104:9301–9306. [PubMed: 17517596]
- Wu MM, Luik RM, Lewis RS. Some assembly required: constructing the elementary units of store-operated Ca²⁺ entry. *Cell calcium* 2007;42:163–172. [PubMed: 17499354]
- Parekh AB, Putney JW Jr. Store-operated calcium channels. *Physiological reviews* 2005;85:757–810. [PubMed: 15788710]
- Vig M, et al. CRACM1 multimers form the ion-selective pore of the CRAC channel. *Curr Biol* 2006;16:2073–2079. [PubMed: 16978865]
- Feske S, et al. A mutation in Orai1 causes immune deficiency by abrogating CRAC channel function. *Nature* 2006;441:179–185. [PubMed: 16582901]
- Mignen O, Thompson JL, Shuttleworth TJ. STIM1 regulates Ca²⁺ entry via arachidonate-regulated Ca²⁺-selective (ARC) channels without store depletion or translocation to the plasma membrane. *The Journal of physiology* 2007;579:703–715. [PubMed: 17158173]

12. Yuan JP, Zeng W, Huang GN, Worley PF, Muallem S. STIM1 heteromultimerizes TRPC channels to determine their function as store-operated channels. *Nature cell biology* 2007;9:636–645.
13. Parvez S, et al. STIM2 protein mediates distinct store-dependent and store-independent modes of CRAC channel activation. *Faseb J.* 2007
14. Ong HL, et al. Dynamic assembly of TRPC1-STIM1-Orai1 ternary complex is involved in store-operated calcium influx. Evidence for similarities in store-operated and calcium release-activated calcium channel components. *The Journal of biological chemistry* 2007;282:9105–9116. [PubMed: 17224452]
15. Huang GN, et al. STIM1 carboxyl-terminus activates native SOC, I(crac) and TRPC1 channels. *Nature cell biology* 2006;8:1003–1010.
16. Hamilton SL. Ryanodine receptors. *Cell calcium* 2005;38:253–260. [PubMed: 16115682]
17. MacLennan DH. Ca²⁺ signaling and muscle disease. *European journal of biochemistry/FEBS* 2000;267:5291–5297. [PubMed: 10951187]
18. Kurebayashi N, Ogawa Y. Depletion of Ca²⁺ in the sarcoplasmic reticulum stimulates Ca²⁺ entry into mouse skeletal muscle fibres. *The Journal of physiology* 2001;533:185–199. [PubMed: 11351027]
19. Rosenberg P, et al. TRPC3 channels confer cellular memory of recent neuromuscular activity. *Proceedings of the National Academy of Sciences of the United States of America* 2004;101:9387–9392. [PubMed: 15199180]
20. Pan Z, et al. Dysfunction of store-operated calcium channel in muscle cells lacking mg29. *Nature cell biology* 2002;4:379–383.
21. Stiber JA, et al. Homer modulates NFAT-dependent signaling during muscle differentiation. *Dev Biol* 2005;287:213–224. [PubMed: 16226241]
22. Chin ER, et al. A calcineurin-dependent transcriptional pathway controls skeletal muscle fiber type. *Genes Dev* 1998;12:2499–2509. [PubMed: 9716403]
23. Williams RS, Rosenberg P. Calcium-dependent Gene Regulation in Myocyte Hypertrophy and Remodeling. *Cold Spring Harb Symp Quant Biol* 2002;LXVII:1–5.
24. Luik RM, Lewis RS. New insights into the molecular mechanisms of store-operated Ca(2+) signaling in T cells. *Trends in molecular medicine* 2007;13:103–107. [PubMed: 17267286]
25. Horsley V, Jansen KM, Mills ST, Pavlath GK. IL-4 acts as a myoblast recruitment factor during mammalian muscle growth. *Cell* 2003;113:483–494. [PubMed: 12757709]
26. Kegley KM, Gephart J, Warren GL, Pavlath GK. Altered primary myogenesis in NFATC3(–/–) mice leads to decreased muscle size in the adult. *Dev Biol* 2001;232:115–126. [PubMed: 11254352]
27. Friday BB, Horsley V, Pavlath GK. Calcineurin activity is required for the initiation of skeletal muscle differentiation. *The Journal of cell biology* 2000;149:657–666. [PubMed: 10791979]
28. Dziadek MA, Johnstone LS. Biochemical properties and cellular localisation of STIM proteins. *Cell calcium.* 2007
29. Yeromin AV, Roos J, Stauderman KA, Cahalan MD. A store-operated calcium channel in *Drosophila* S2 cells. *The Journal of general physiology* 2004;123:167–182. [PubMed: 14744989]
30. Prakriya M, Lewis RS. Separation and characterization of currents through store-operated CRAC channels and Mg²⁺-inhibited cation (MIC) channels. *The Journal of general physiology* 2002;119:487–507. [PubMed: 11981025]
31. Mercer JC, et al. Large store-operated calcium selective currents due to co-expression of Orai1 or Orai2 with the intracellular calcium sensor, Stim1. *The Journal of biological chemistry* 2006;281:24979–24990. [PubMed: 16807233]
32. Prakriya M, Lewis RS. CRAC channels: activation, permeation, and the search for a molecular identity. *Cell calcium* 2003;33:311–321. [PubMed: 12765678]
33. Prakriya M, et al. Orai1 is an essential pore subunit of the CRAC channel. *Nature* 2006;443:230–233. [PubMed: 16921383]
34. Smyth JT, et al. Emerging perspectives in store-operated Ca²⁺ entry: roles of Orai, Stim and TRP. *Biochimica et biophysica acta* 2006;1763:1147–1160. [PubMed: 17034882]
35. Launikonis BS, Rios E. Store-operated Ca²⁺ entry during intracellular Ca²⁺ release in mammalian skeletal muscle. *The Journal of physiology* 2007;583:81–97. [PubMed: 17569733]

36. Eu JP, et al. Concerted regulation of skeletal muscle contractility by oxygen tension and endogenous nitric oxide. *Proceedings of the National Academy of Sciences of the United States of America* 2003;100:15229–15234. [PubMed: 14645704]
37. MacLennan DH. Interactions of the calcium ATPase with phospholamban and sarcolipin: structure, physiology and pathophysiology. *Journal of muscle research and cell motility* 2004;25:600–601. [PubMed: 16118852]
38. Lorenzon P, Giovannelli A, Ragozzino D, Eusebi F, Ruzzier F. Spontaneous and repetitive calcium transients in C2C12 mouse myotubes during in vitro myogenesis. *Eur J Neurosci* 1997;9:800–808. [PubMed: 9153587]
39. Lorenzon P, Grohovaz F, Ruzzier F. Voltage- and ligand-gated ryanodine receptors are functionally separated in developing C2C12 mouse myotubes. *The Journal of physiology* 2000;525(Pt 2):499–507. [PubMed: 10835050]
40. Chun LG, Ward CW, Schneider MF. Ca²⁺ sparks are initiated by Ca²⁺ entry in embryonic mouse skeletal muscle and decrease in frequency postnatally. *American journal of physiology* 2003;285:C686–697. [PubMed: 12724135]
41. Konig S, Beguet A, Bader CR, Bernheim L. The calcineurin pathway links hyperpolarization (Kir2.1)-induced Ca²⁺ signals to human myoblast differentiation and fusion. *Development (Cambridge, England)* 2006;133:3107–3114.
42. Philipp S, et al. TRPC3 mediates T-cell receptor-dependent calcium entry in human T-lymphocytes. *The Journal of biological chemistry* 2003;278:26629–26638. [PubMed: 12736256]
43. Lopez JJ, Salido GM, Pariente JA, Rosado JA. Interaction of STIM1 with endogenously expressed human canonical TRP1 upon depletion of intracellular Ca²⁺ stores. *The Journal of biological chemistry* 2006;281:28254–28264. [PubMed: 16870612]
44. Mallouk N, Jacquemond V, Allard B. Elevated subsarcolemmal Ca²⁺ in mdx mouse skeletal muscle fibers detected with Ca²⁺-activated K⁺ channels. *Proceedings of the National Academy of Sciences of the United States of America* 2000;97:4950–4955. [PubMed: 10781103]
45. Whitehead NP, Streamer M, Lusambili LI, Sachs F, Allen DG. Streptomycin reduces stretch-induced membrane permeability in muscles from mdx mice. *Neuromuscul Disord* 2006;16:845–854. [PubMed: 17005404]
46. Suchyna TM, Sachs F. Mechanosensitive channel properties and membrane mechanics in mouse dystrophic myotubes. *The Journal of physiology* 2007;581:369–387. [PubMed: 17255168]
47. Lorin-Nebel C, Xing J, Yan X, Strange K. CRAC channel activity in *C. elegans* is mediated by Orai1 and STIM1 homologues and is essential for ovulation and fertility. *The Journal of physiology* 2007;580:67–85. [PubMed: 17218360]
48. Yan X, et al. Function of a STIM1 homologue in *C. elegans*: evidence that store-operated Ca²⁺ entry is not essential for oscillatory Ca²⁺ signaling and ER Ca²⁺ homeostasis. *The Journal of general physiology* 2006;128:443–459. [PubMed: 16966474]
49. Vig M, et al. Defective mast cell effector functions in mice lacking the CRACM1 pore subunit of store-operated calcium release-activated calcium channels. *Nature immunology* 2008;9:89–96. [PubMed: 18059270]
50. Mohler PJ, Gramolini AO, Bennett V. The ankyrin-B C-terminal domain determines activity of ankyrin-B/G chimeras in rescue of abnormal inositol 1,4,5-trisphosphate and ryanodine receptor distribution in ankyrin-B (–/–) neonatal cardiomyocytes. *The Journal of biological chemistry* 2002;277:10599–10607. [PubMed: 11781319]

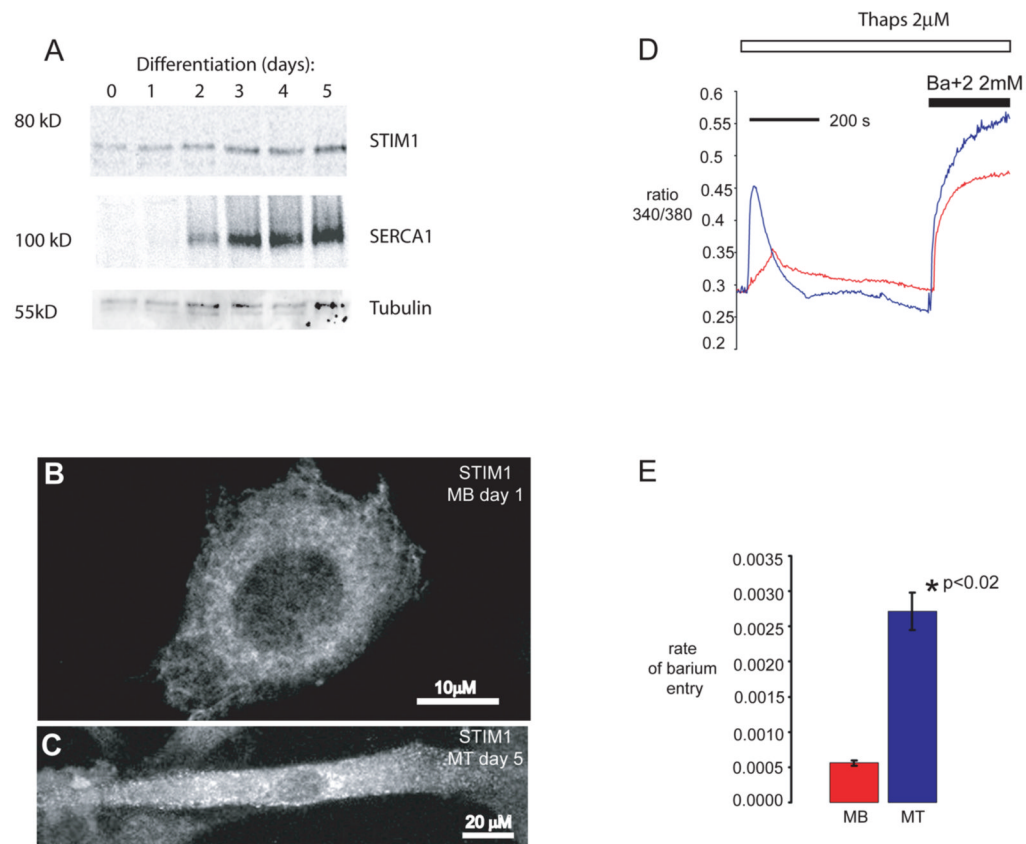


Figure 1. Muscle differentiation is associated with increased expression of STIM1 and redistribution of STIM1

A) Differentiating C₂C₁₂ cells were harvested at the indicated times and protein lysates were separated by SDS-PAGE and immunoblotted for STIM1 and SERCA1 using specific antibodies. Complete scans of these gels are shown in supplemental information (supplemental fig 6). B) STIM1 expression in C₂C₁₂ myoblasts (MB, scale bar = 10 μm) and C) in C₂C₁₂ cells allowed to differentiate into myotubes (MT, scale bar = 20 μm). STIM1 aggregation and redistribution to the cellular periphery occurs during myogenesis. Arrows represent peripherally localized STIM1. D) Store-operated calcium entry was greater in myotubes than in myoblasts. Fura-2 loaded C₂C₁₂ myoblasts and myotubes were placed in zero calcium media, and treated with thapsigargin to induce store depletion and verapamil to inhibit L-type Ca²⁺ channels. Once cytoplasmic Ca²⁺ returned to baseline, barium was added to the extracellular medium as a surrogate for Ca²⁺. Representative average tracings of individual myoblasts and myotubes showed a significant increase in store-operated influx in myotubes. E) The rate of store-operated barium influx, calculated by the first derivative of the 340/380 nm ratio in the first 100 seconds of influx, was $5.57 \times 10^{-4} \pm 4 \times 10^{-5}$ arbitrary unit/sec (n = 23) in myoblasts, and $2.72 \times 10^{-3} \pm 3 \times 10^{-4}$ arbitrary unit/sec (n = 6) in myotubes (p < 0.001). The data shown represent the mean ± SE.

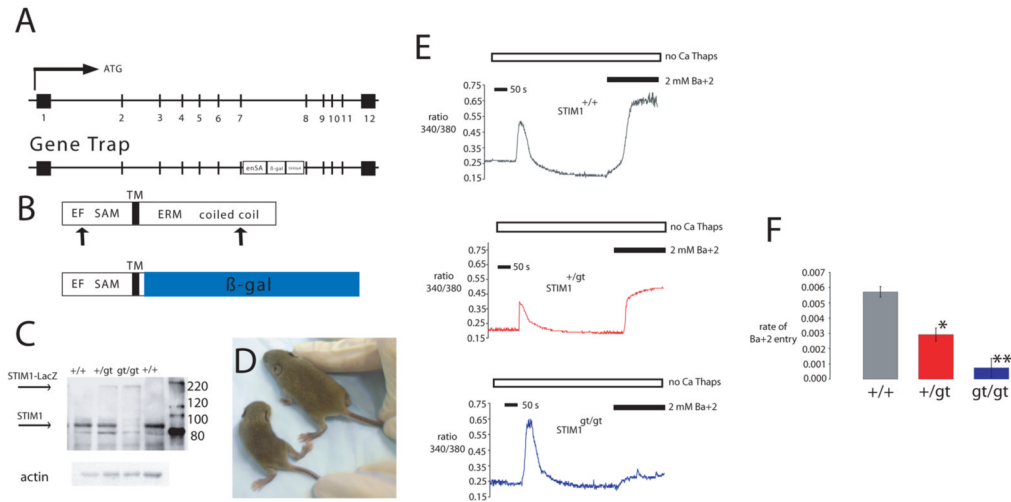


Figure 2. Gene trap strategy for STIM1

A) Mouse STIM1 gene showing the exon structure in boxes (upper panel). Corresponding STIM1 locus with gene trap vector insertion (lower panel). The gene trap vector carries the engrailed2 intron (en2) and splice acceptor site (SA), β -galactosidase reporter gene and a SV40 polyadenylation site (SV40pA) inserted between exons 7 and 8. B) Both WT and gene-trapped STIM1 protein contain the EF hands and SAM domain of the N-terminus that localizes to the ER lumen, and the membrane spanning region (TM). The cytosolic loop is depicted at the C-terminus only in the WT locus as the gene trap product fuses the first 30 amino acids of STIM1 N-terminus to β -gal. C) Lysates prepared from muscles of WT, +/gt, and gt/gt mice and immunoblotted for STIM1 revealed WT STIM1 and STIM1 fusion protein. Complete scans of these gels are shown in supplemental information (supplemental Fig 6). D) Two week old gt/gt mice appeared smaller and weaker compared to WT littermates. (STIM1gt/gt is seen on the left.) E–F) Store-operated calcium entry in primary myotubes prepared from WT, +/gt, and gt/gt mice. Fura-2 loaded primary myotubes were placed in zero calcium media, and treated with thapsigargin to induce store depletion and verapamil to inhibit L-type Ca^{2+} channels. Once cytoplasmic Ca^{2+} returned to baseline, barium was added to the extracellular medium as a surrogate for Ca^{2+} . Representative average tracings of individual myotubes showed a significant decrease in store-operated influx in +/gt and gt/gt myotubes compared with myotubes prepared from WT littermate controls, with minimal influx in gt/gt myotubes.

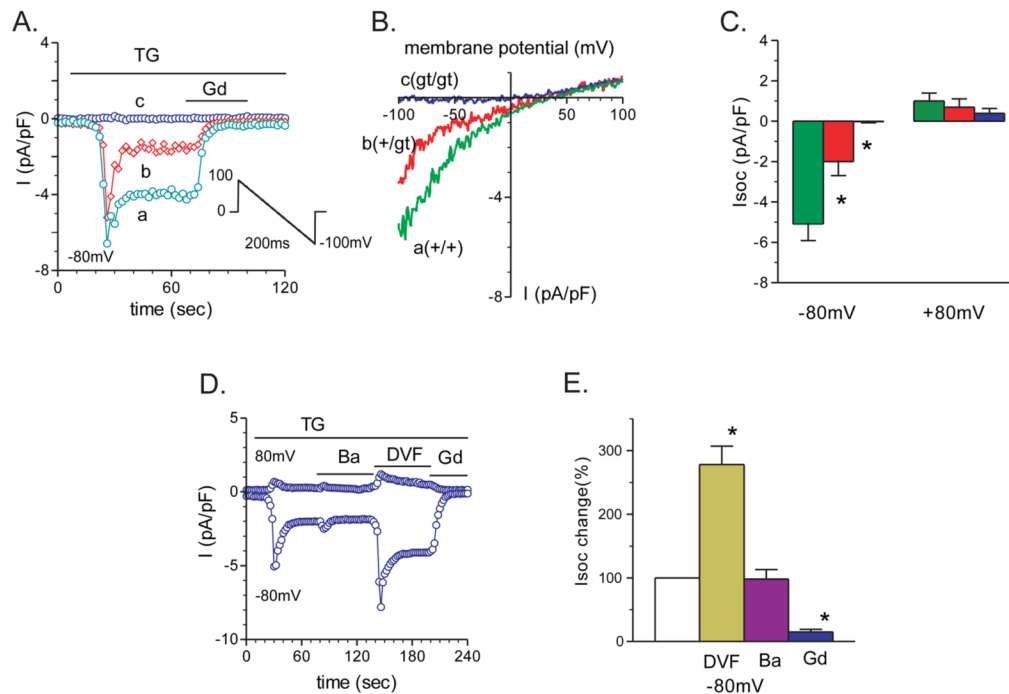


Figure 3. Store depletion fails to activate SOC current in primary myotubes lacking functional STIM1

SOC currents in response to TG ($2\mu\text{M}$) were recorded from myotubes prepared from $\text{STIM1}^{\text{gt/gt}}$, $\text{STIM1}^{+/gt}$, and $\text{STIM1}^{+/+}$ mice. A) Examples of thapsigargin (TG)-induced I_{soc} responses in $\text{STIM1}^{\text{gt/gt}}$, $+/gt$, and $+/+$ myotubes. The currents were induced by a 200ms voltage ramp protocol (1mV/ms), from 100mV to -100mV , from a holding potential of 0mV (see inset). Sweeps occurred every 2 seconds. Peak I_{soc} was leak-subtracted and normalized by membrane capacitance. I_{soc} current density was measured at -80mV . Store-depletion resulted in a large I_{soc} peak in $\text{STIM1}^{+/+}$ myotubes (green trace) and a smaller I_{soc} response in $\text{STIM1}^{+/gt}$ myotubes (red trace), but no significant response in $\text{STIM1}^{\text{gt/gt}}$ (blue trace) myotubes. I_{soc} was inhibited rapidly after the addition of gadolinium (Gd^{3+} , $100\mu\text{M}$). B) I/V plots of the I_{soc} currents after TG perfusion at the times indicated in A) of $\text{STIM1}^{+/+}$ (a, green trace), $\text{STIM1}^{+/gt}$ (b, red trace), $\text{STIM1}^{\text{gt/gt}}$ (c, blue trace). Note the stimulatory effect of TG was absent in $\text{STIM1}^{\text{gt/gt}}$ myotubes. C) Group mean values of peak I_{soc} at -80mV and $+80\text{mV}$ in $\text{STIM1}^{+/+}$ ($n=19$), $\text{STIM1}^{+/gt}$ ($n=8$), vs. $\text{STIM1}^{\text{gt/gt}}$ ($n=8$) myotubes; *, $P<0.05$, $\text{STIM1}^{\text{gt/gt}}$ vs. $\text{STIM1}^{+/+}$, and $\text{STIM1}^{+/gt}$ myotubes. D) An example of TG-induced I_{soc} response at $+80\text{mV}$ and -80mV in solutions containing Ca^{2+} , Ba^{2+} , divalent-free (DVF), and Gd^{3+} containing solutions respectively. E) Group mean changes of peak I_{soc} at -80mV in the presence of Ba^{2+} (maroon bar, $n=12$), DVF (yellow bar, $n=10$), and Gd^{3+} (blue bar, $n=9$) containing external solutions. Open bars represent control I_{soc} (100%). *, $P<0.05$, control versus Ba^{2+} , DVF, or with Gd^{3+} .

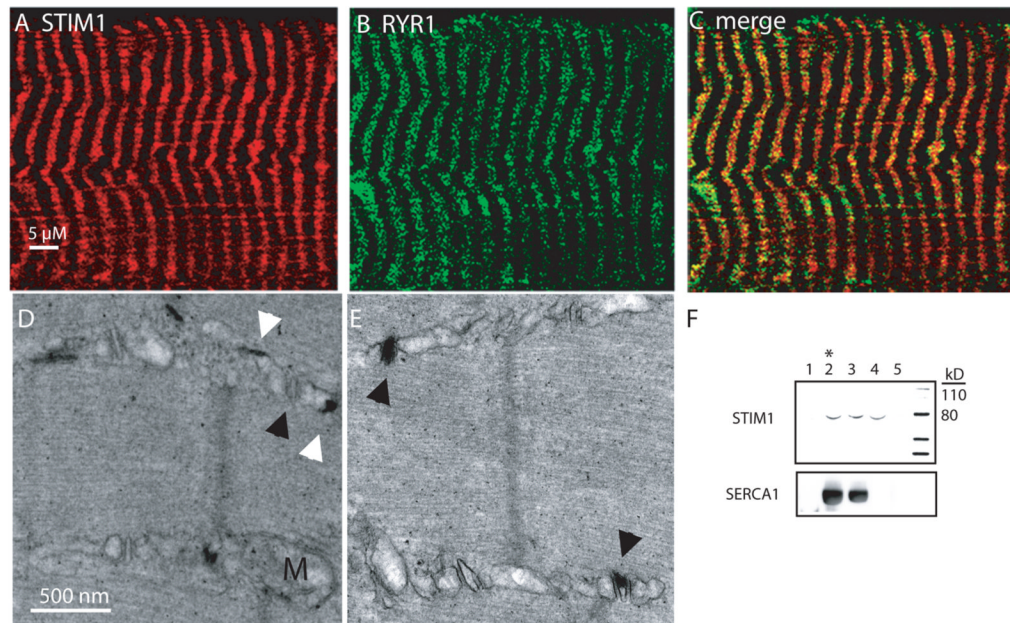


Figure 4. STIM1 Localization

A) Immunostaining for STIM1 in skeletal muscle using a STIM1 specific antibody displayed a striated pattern. B) Immunostaining for RYR. C) Merged panel shows partial overlap of STIM1 and RYR. Scale bar (A–C) = 5 μm. D–E) Expression of the STIM1-LacZ fusion protein by electron microscopy. Aggregates of the reaction products of beta-galactosidase were detected in the longitudinal SR (white arrowhead) as well as the junction of the t-tubule and terminal SR (black arrowhead). Scale bar (D–E) = 500 nm. F) Isolated microsomal fractions were obtained using sucrose gradients from rabbit muscle which revealed the absence of STIM1 expression in the fraction corresponding to the contractile proteins and debris (1), and the presence of STIM1 expression in the terminal cisternae (2), longitudinal SR (2 and 3), and t-tubular fractions (4 and 5). * indicates fraction with greatest $[H^{3+}]$ RYR binding. Complete scans of these gels are shown in supplemental information (supplemental Fig 6).

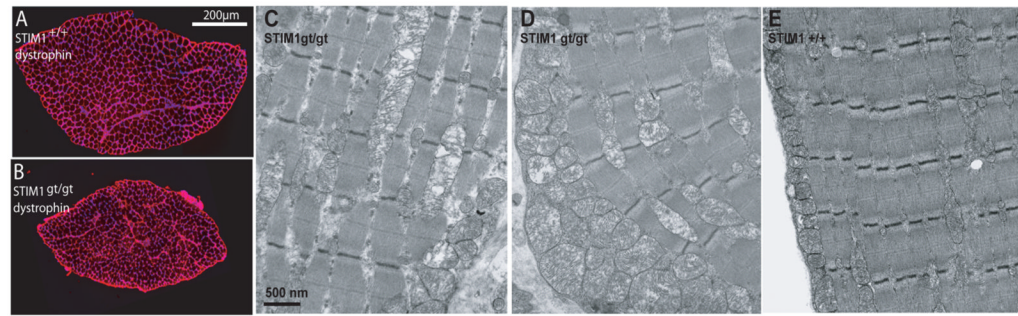


Figure 5. Mice without functional STIM1 display a neonatal skeletal myopathy

A–B) Dystrophin immunostaining of cross sections taken from neonatal muscle of STIM1^{+/+} and STIM1^{gt/gt} mice. Nuclei were counterstained with DAPI. Scale bar = 200 μm. C–E) Transmission electron microscopy was used to examine muscle ultrastructure from STIM1^{gt/gt} (C and D) and STIM1^{+/+} mice (E). TA muscles were taken from 7–10 day old STIM1^{+/+} and STIM1^{gt/gt} mice. 5000X images were obtained from muscles of two mice. Scale bar = 500 nM.

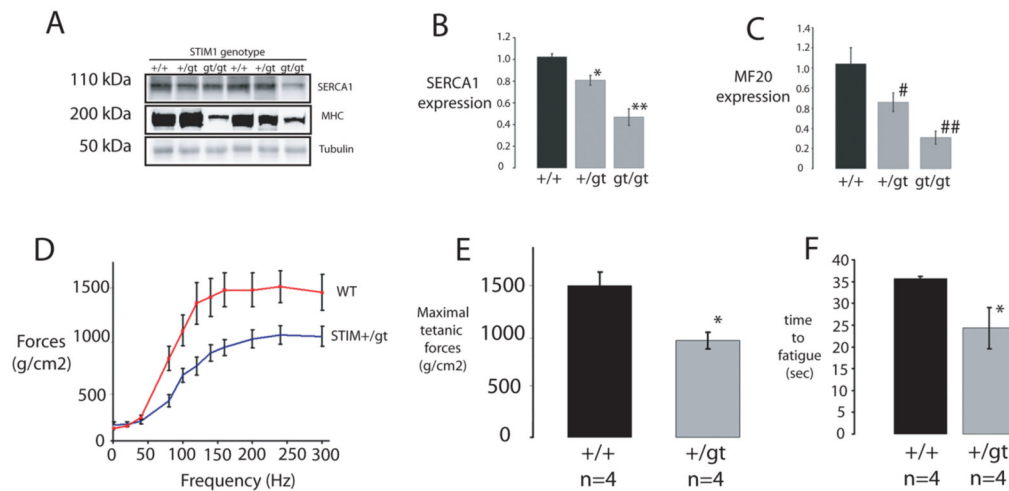


Figure 6. Muscle gene expression and functional analysis of mutant STIM1 mice

A–C) Muscle protein lysates taken from neonatal mice ($STIM1^{gt/gt}$, $STIM1^{+/gt}$ versus $STIM1^{+/+}$) displayed a reduction in SERCA1 (top panel) and Myosin Heavy Chain (middle panel) in mutant STIM1 mice as assessed by immunoblotting with specific antibodies for SERCA1 and MHC (MF20). Quantification using densitometry is provided for studies of three mice for each genotype for SERCA1 (B) and MHC (C). Complete scans of these gels can be found in supplemental information (supplemental Fig 6). D) Contractile force measurements after tetanic stimulation of EDL muscles taken from $STIM1^{+/gt}$ ($n=4$) and $STIM1^{+/+}$ mice ($n=4$). E) Bar graphs represents maximal forces (mean \pm SE) following tetanic stimulation for $STIM1^{+/gt}$ and $STIM1^{+/+}$. F) Bar graph of time to fatigue after repetitive stimulation for muscles taken from $STIM1^{+/gt}$ and $STIM1^{+/+}$ mice. Time to fatigue was measured using a protocol of one 100Hz stimulation per sec, for a duration of 200ms. Values (mean \pm SE) represent the time required for a decay in force generation to 50% maximal force, following stimulation of 4 muscles from each genotype.

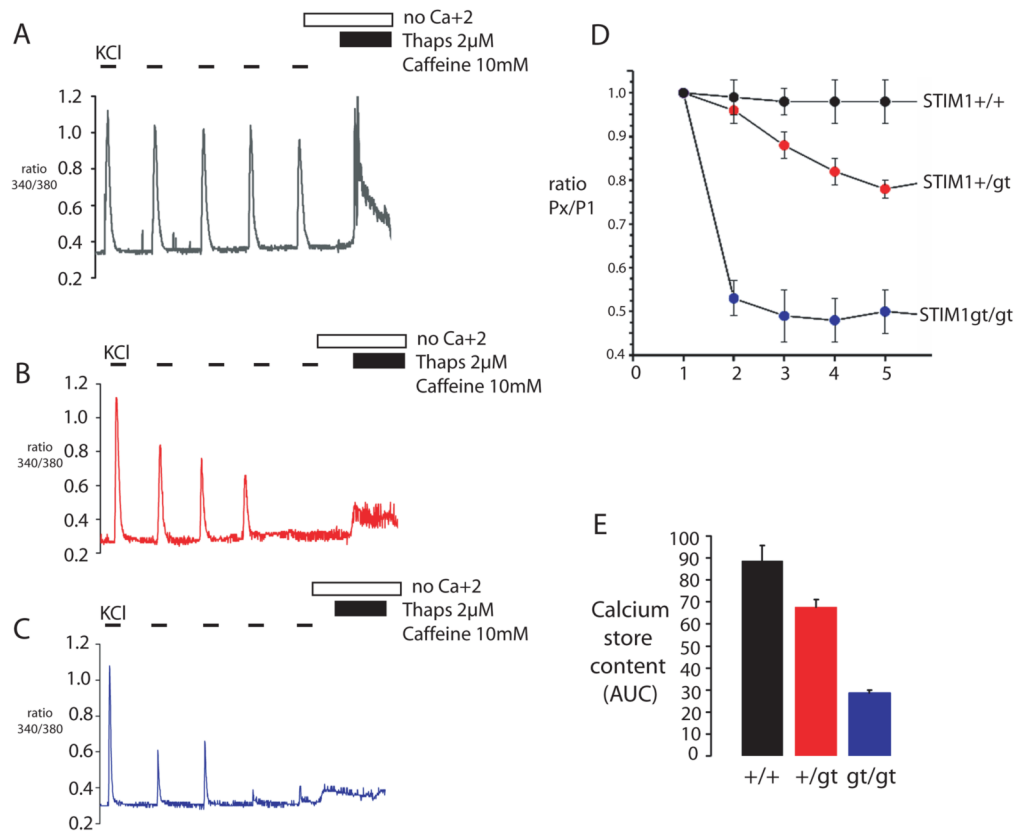


Figure 7. STIM1 mediated store refilling is required for fatigue resistance in skeletal myotubes
 A–C) Calcium transients were measured from STIM1^{+/+} (A), STIM1^{+/gt} (B) and STIM1^{gt/gt} (C) myotubes by a series of KCl pulses (55mM) in the presence of [Ca²⁺]_o. SR store content was then determined by stimulating myotubes in a zero [Ca²⁺]_o solution with TG (2μM) and caffeine (10mM). D) STIM1^{+/+} myotubes responded to a series of KCl stimulations with little change in the amplitude of the calcium transient (black trace). STIM1^{+/gt} (red trace) and STIM1^{gt/gt} (blue trace) myotubes responded to the series of KCl-pulses with a decrement in peak amplitude of the calcium transient as measured by the ratio of the amplitude of subsequent KCl pulses to the initial KCl pulse (P_X/P₁). E) Calcium store content after KCl stimulation in STIM1^{+/+}, STIM1^{+/gt} and STIM1^{gt/gt} myotubes. Data shown represent mean ± SE.

Table 1

Analysis of offspring from intercrossed heterozygotes

Number of offspring of each genotype are indicated for observed and expected numbers (parentheses) based on Mendelian ratios of 1:2:1.

Age	+/+	+/gt	gt/gt	total	X ²	p
Embryo	10 (8.25)	15 (16.25)	7 (8.25)	33	0.3	NS
Neonates	34 (26.75)	61 (53.5)	12 (26.75)	107	6.97	<0.003
3 weeks postpartum	36 (33.25)	94 (66.5)	3 (33.25)	133	30.38	<0.001